Title: Automated cot-side tracking of functional brain age in preterm infants with routine EEG monitoring

Authors: Nathan J. Stevenson[1]*, Lisa Oberdorfer[2], Maria-Luisa Tataranno[3], Michael Breakspear[1,4], Paul B. Colditz[5], Linda S. de Vries[3], Manon J. N. L. Benders[3], Katrin Klebermass-Schrehof[2], Sampsa Vanhatalo[6], James A. Roberts[1]

Affiliations:

[1] QIMR Berghofer Medical Research Institute, Brisbane, QLD 4006, Australia

[2] Department of Pediatrics, Division of Neonatology, Pediatric Intensive Care and Neuropediatrics, Medical University of Vienna, Austria

[3] Department of Neonatology, University Medical Center Utrecht, Utrecht, The Netherlands

[4] Priority Research Center for Mind and Brain, University of Newcastle, Newcastle, NSW 2305, Australia

[5] Centre for Clinical Research, Faculty of Medicine, University of Queensland, Brisbane, QLD 4029, Australia

[6] Department of Children's Clinical Neurophysiology, BABA center, Pediatric Research Center, Children's Hospital, HUS Medical Imaging Center, Helsinki University Central Hospital, University of Helsinki, Finland

*** Corresponding Author:** nathan.stevenson@qimrberghofer.edu.au

Abstract

A major challenge in the care of preterm infants is the early identification of compromised neurological development. While several measures are routinely used to track anatomical growth, there is a striking lack of reliable and objective tools for tracking maturation of early brain function; a cornerstone of lifelong neurological health. We present a cot-side method for measuring the functional maturity of the newborn brain based on routinely-available neurological monitoring with electroencephalography (EEG). We used a dataset EEG recordings from 65 infants to train a multivariable prediction of functional brain age (FBA) from EEG. Using machine learning on traditional and recently-developed computational EEG measures yielded an FBA that correlated strongly with the postmenstrual age of an infant. Moreover, individual babies follow well-defined individual trajectories. We validated the FBA predictor on independent data from a different site with different recording configuration. In a subgroup of infants with repeated EEG recordings, a persistently negative predicted age difference was associated with poor neurodevelopmental outcome. The FBA enables the tracking of functional neurodevelopment in preterm infants. Functional age assessment can be used to assist clinical management and identify infants who will benefit most from early intervention.

Keywords: neuro-monitoring, brain age, EEG, predicted age difference, preterm infants

Introduction

Preterm birth is a substantial risk to infant health. While mortality rates have dropped considerably over recent years due to improvements in clinical care, these infants remain at significant risk of neurodevelopmental delay and a host of other chronic impairments in later life (*1-3*). It is therefore of critical importance to reduce the exposure of the preterm infant to neurological adversities while in the neonatal intensive care unit (NICU), and to identify those infants who will benefit most from early intervention (*4*). Recent advances in neurological care have stressed the need for improving early functional biomarkers of neurodevelopment to expedite cycles within clinical intervention trials.

Monitoring physiological and anatomical growth is crucial for clinicians when optimizing the care of very or extremely preterm infants. Critical time periods for the direction of care are usually the first days after birth, the time of discharge from tertiary care to step-down units, as well as the follow-up visit at near term-equivalent age. The EEG is the best available tool for cot-side assessment of brain function, and it is widely used for early therapeutic decisions as well as the prediction of neurodevelopmental outcome in preterm infants (*5-9*). However, the clinical use of EEG in the NICU is complicated by difficulties in interpretation and the availability of expertise to perform interpretation (*10*). Computer-assisted analysis presents an opportunity to solve both problems by providing simplified EEG measures that can be interpreted by clinical staff, on demand and in real time.

Assessing brain maturity via the visual interpretation of the EEG during an infant's stay in the NICU has been a part of clinical practice for decades (*11*). Its use complements traditional anatomical measures such as weight, length, and head circumference. A lag between estimated functional brain age (FBA) and the chronological age of the individual – the predicted age difference (PAD) – holds potential as a functional biomarker. It is crucial that the FBA is highly correlated with chronological age to ensure that claims of 'dysmaturity' are valid and not simply alternate manifestations of dysfunction or pathology. The concept of measuring PAD has recently attracted interest for the diagnosis of a wide variety of neurological pathologies over a wide range of ages (*12*). We have previously shown that it is possible to construct computational measures that emulate many visually observed EEG phenomena such as inter-burst interval, synchrony, discontinuity, and frequency content. The combination of these computational measures can predict the EEG maturation of the brain with a high degree of accuracy (*13, 14*).

While 'computerizing' visual classification of EEG phenomena is a useful initial stage, it suffers from two shortcomings. First, it is limited by the visual interpretation of EEG characteristics and, therefore, lacks a robust physiological, physical, and technical foundation. Second, it is inherently susceptible to a myriad of confounders that arise from the relationship between conventionally-recognized EEG phenomenology and technical recording traditions. Recent advances in computational neuroscience suggest that the EEG contains markers of brain function that are not readily discernible by visual EEG review (*15-19*). Key information lies within the widespread network of intermittent bursting that dominates early cortical activity (*20, 21*). This developmentally unique activity is known to be crucial for supporting neuronal growth and guiding early brain wiring (*22, 23*). It changes rapidly over the last trimester, is sensitive to exogenous disturbances, and is predictive of future neurodevelopment (*24-26*).

We recently showed that bursting activity possesses the statistical properties of crackling noise (*15, 27*), a form of complex, non-Gaussian noise that occurs when there is a critical balance between amplifying (excitatory) and dissipating (inhibitory) influences within a system (brain) (*28*). Measures of this noise have been shown to be able to detect neurological challenge in preterm and term neonates (*25, 29, 30*). Here, we applied signal analysis methods derived from the analysis of crackling noise to the assessment of early brain maturation, alongside other EEG metrics. Initially, we assessed the accuracy of single variable models to predict PMA. We then built a multivariable model of PMA, trained using machine learning techniques, to yield an estimate of FBA. We validated the subsequent FBA on an independent dataset to address issues of reproducibility and robustness of the method to other EEG recording settings and environments. Finally, we evaluated the applicability of the difference between FBA and PMA (a predicted age difference) as a predictor of neurodevelopmental outcome in a subgroup of infants with multiple, serial recordings.

Results

The aim of this study was to determine the efficacy of automated EEG analysis for the assessment of PMA in preterm infants. This study employed two different datasets of serial EEG recordings of preterm infants recorded from NICUs in different countries. The first dataset (recorded in Vienna: 65 infants, 177 EEG recordings) was used to train and evaluate the FBA measure, as well as investigate the use of FBA as a predictor of neurodevelopmental outcome (Fig. 1). The second dataset (recorded in Utrecht: 42 infants, 99 EEG recordings) was used to validate the FBA measure trained on the first dataset. Infants were born before 29 weeks

gestation, with EEG recorded serially at 25-39 weeks PMA (Vienna) or 25-34 weeks PMA (Utrecht). We used machine learning techniques to form an estimate of FBA using quantitative EEG (qEEG) variables that can be grouped into three categories: phenomenological analysis, burst analysis, and other recently-developed analyses (Fig. S1 and Table S1).

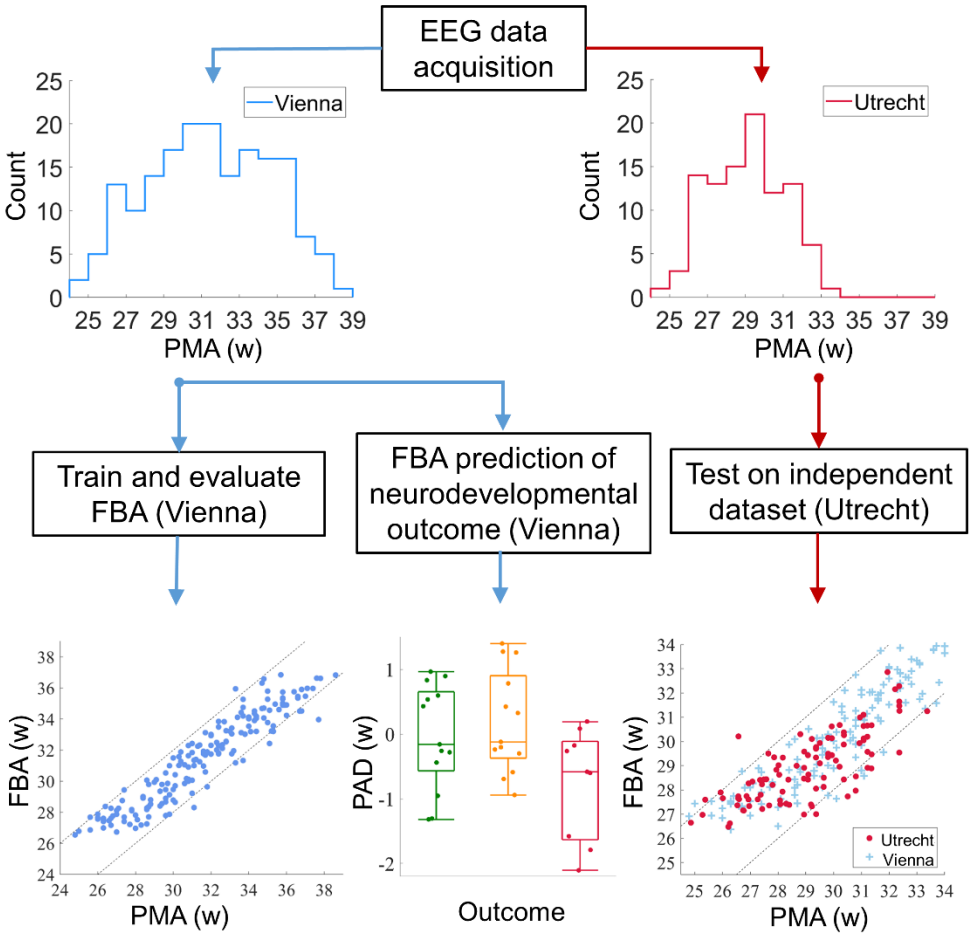

Figure 1: Data acquisition, training, evaluation and testing of the FBA. The histograms depict the distribution of EEG recordings with PMA (in weeks) in each dataset. The bottom row illustrates the analyses corresponding to each dataset. PAD is the predicted age difference between functional brain age (FBA) and post-menstrual age (PMA).

PMA prediction using a single variable FBA

Across all metrics tested, the qEEG variable that had the highest correlation with PMA was the asymmetry of average burst shape (Fig. 2A), which exhibits a strong linear relationship with bursts becoming more symmetric with increasing PMA (Fig. 2B). Several additional qEEG variables were strongly associated with PMA (see Table S1 of the supplementary

Information). Metrics that were not reliably predictive of PMA were varied in nature and included several relative band powers and measures of burst duration.

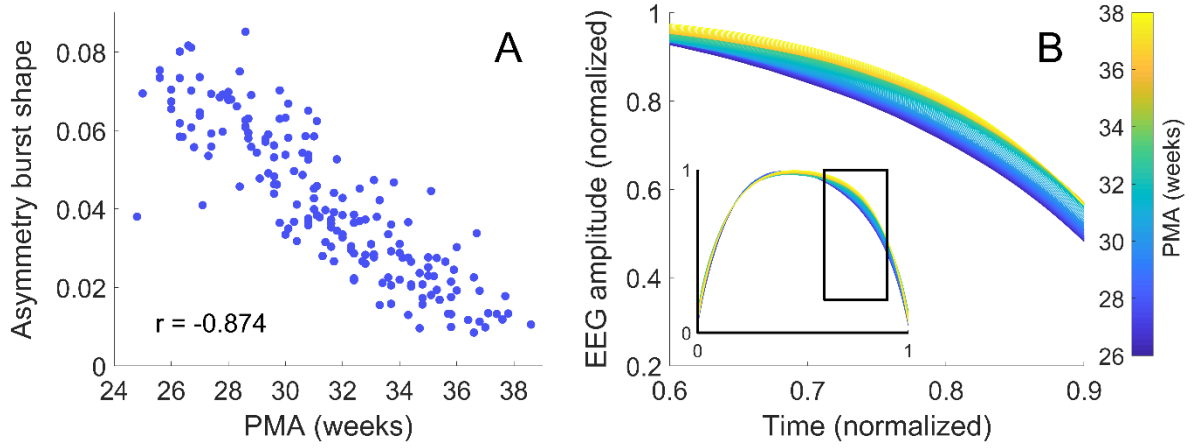

Figure 2. Changes in burst characteristics with post-menstrual age (PMA). (**A**) Asymmetry of average burst shape versus PMA (*r* is Pearson's linear correlation coefficient). (**B**) Average burst shape of the EEG amplitude grouped according to PMA with fortnightly steps from 25 weeks; the inset shows the entire average burst. The changes seen in (B) are best represented by measures of burst asymmetry.

PMA prediction using the multivariable FBA

Combining several qEEG variables into a multivariable model improves the prediction accuracy of the FBA (Table 1). Assessed within a leave-one-out cross-validation, the multivariable FBA model had a significantly higher correlation with PMA than a single variable model based on the single best variable (asymmetry of the burst shape) for models based on bursts, phenomenological, and other newly proposed qEEG variables (Δr = 0.109, 95% CI: 0.059 to 0.162; Δr = 0.095, 95% CI: 0.045 to 0.150; Δr = 0.094, 95% CI: 0.057 to 0.142; n = 177, respectively). The multivariable model using burst qEEG variables also had a significantly higher correlation with PMA than multivariable models based on phenomenological or other newly proposed qEEG variables (Δr = 0.030, 95% CI: 0.001 to 0.062; Δr = 0.027, 95% CI: 0.005 to 0.049; n = 177, respectively).

Incorporating qEEG variables into a multivariable model, via a variable selection procedure, further improved the accuracy of the FBA (Table 1). The FBA estimator identified PMA to within 2 weeks for 90% of recordings, with a median absolute error of 0.7 weeks. A scatter plot of FBA versus PMA exhibits a clear linear trend (Fig. 3A), with a tight clustering of FBA within ±2 weeks of the PMA. The performance of this FBA, which contained a mixture of

burst, phenomenological, and other recently-developed EEG variables, was significantly higher than multivariable models based on only phenomenological analysis, burst analysis or other analyses alone (Δr = 0.045, 95%CI: 0.020 to 0.073; Δr = 0.015, 95%CI: 0.002 to 0.028; and Δr = 0.042, 95%CI: 0.024 to 0.063, respectively; n = 177). Variable selection resulted in a median of 53 variables (IQR; 49-55; n = 65 folds). In general, the most commonly selected variables were burst shape (asymmetry, sharpness), burst number, relative spectral power, activity synchrony index, path length, multi-scale entropy, EEG amplitude envelope, and inter-burst interval – see the Supplementary Information for a complete list of variables and their selection frequencies (Table S1 and Fig. S2).

Table 1: The performance of several multivariable FBA models for predicting PMA in preterm infants on training (cross-validation) and validation datasets. r is the correlation coefficient, n is the number of recordings included in analysis, m is the number of qEEG variables used in the model (for variable selection this is the median number across folds of the cross-validation), 95% CI is the 95th percentile of the confidence interval, IQR is inter-quartile range.

	r (95%CI)	bias (weeks)	variance (weeks)	absolute difference (weeks)	±1 week (%)	±2 weeks (%)
Phenomenological (n = 177; m = 46)	0.894 [0.859-0.919]	-0.1	2.1	0.9 [0.4-1.6]	55	83
Other (n = 177; m = 10)	0.896 [0.866-0.920]	-0.1	2.1	0.9 [0.5-1.5]	53	84
Bursts (n = 177; m = 40)	0.923 [0.905-0.940]	-0.2	1.6	0.9 [0.3-1.4]	60	89
Variable Selection (n = 177; m = 53)	0.938 [0.922-0.952]	-0.1	1.3	0.7 [0.4-1.3]	63	90
Validation: Vienna (n = 134; m = 53)	0.900 [0.873-0.929]	-0.2	1.1	0.6 [0.3-1.2]	64	92
Validation: Utrecht (n = 99; m = 53)	0.765 [0.665-0.846]	0.1	1.5	0.9 [0.4-1.3]	61	90

Validation of FBA on an independent dataset

To directly address the generalizability of our results, we validated the multivariable model in an independent dataset. We found that the multivariable model trained on Vienna data (evaluated via cross-validation) and applied to the Utrecht dataset performs near physiological limits in prediction accuracy, with 90% of epochs correctly identified to within ±2 weeks (Table 1). The absolute error between the FBA and PMA (accuracy), when applied to the Utrecht data, was equivalent to the cross-validation results from the Vienna dataset across a similar range of PMA (Fig. 3B: $p < 0.001$; TOST, equivalence boundary of ±0.5 weeks).

FBA for tracking individual growth and predicting neurodevelopmental outcomes

The accuracy of FBA in tracking cot-side development raises the idea that FBA may be useful for individualized assessment of functional maturity. We used linear mixed modelling to account for serial recordings from individual infants which resulted in an adjusted correlation of $r = 0.978$ (95%CI: 0.974-0.987; $n = 65$). The improvement in correlation over a point-wise estimate implies that individual infant trajectories are more highly correlated with PMA than the cohort average. In other words, infants tend to follow their individual growth trajectories (Fig. 4A), and the FBA is able to track these trajectories with high accuracy.

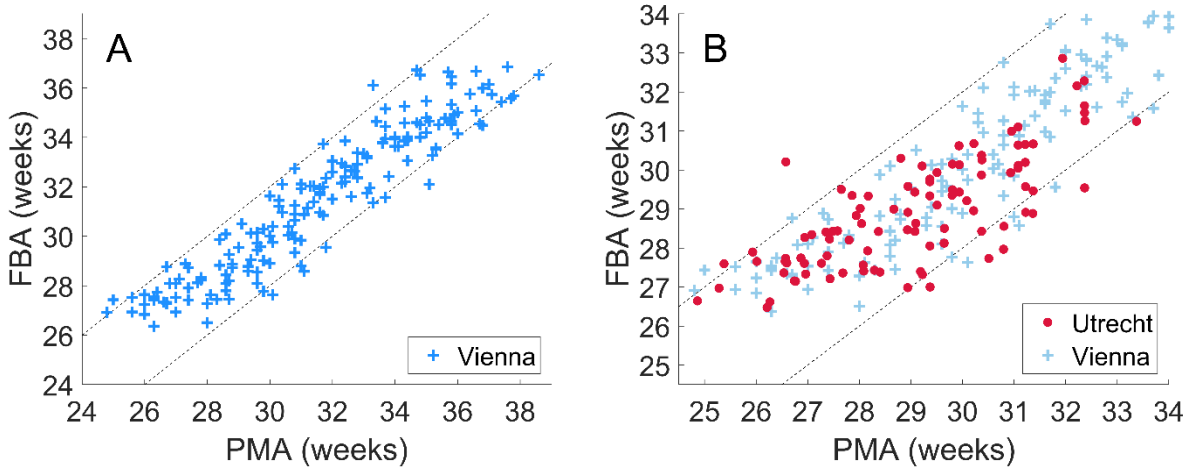

Figure 3: The correlation between a multivariable FBA and chronological age (PMA). (**A**) The multivariable FBA, with variable selection, evaluated on the Vienna dataset via leave-one-subject-out cross-validation over the full range of EEG recording PMAs (24-38 weeks). (**B**) The multivariable FBA trained on the Vienna dataset and applied to an independent dataset recorded from Utrecht over the full range of EEG recording PMAs from the Utrecht dataset (24-34 weeks). Dashed lines denote ±2 weeks difference between FBA and PMA.

growth trajectories as a predictor of neurodevelopmental outcome. In a subgroup of infants with more than two serial recordings (a median PMA range of 6.2 weeks, IQR: 4.6 to 7.5 weeks; Fig. 4B), the average predicted age difference (PAD: difference between FBA and PMA) was significantly associated with neurodevelopmental outcome (One-way ANOVA: F statistic = 3.980, df = 2, $p = 0.029$; $n = 35$, 3 groups: normal, mildly abnormal, abnormal – see Fig. 4C; group variances were homogenous; Levene's Test: $p = 0.82$). Infants with abnormal outcome ($n = 9$) had a PAD that was significantly less than infants with mildly abnormal outcome ($n = 13$) (Cohen's D = 1.12, $p = 0.025$, corrected for multiple comparisons using Tukey's Range Test). The estimated PAD in these infants was also significantly below 0 weeks (t-test: Cohen's D = 0.661, $p = 0.035$; $n = 9$) suggesting a persistent delay in brain maturation (i.e., negative PAD) in infants with abnormal outcome. These differences were not apparent

when including infants with less than three serial EEG recordings (ANOVA: F statistic = 0.0112, df = 2, $p = 0.894$; $n = 54$), suggesting that multiple recordings may be required to assess a PAD associated with neurodevelopmental outcome.

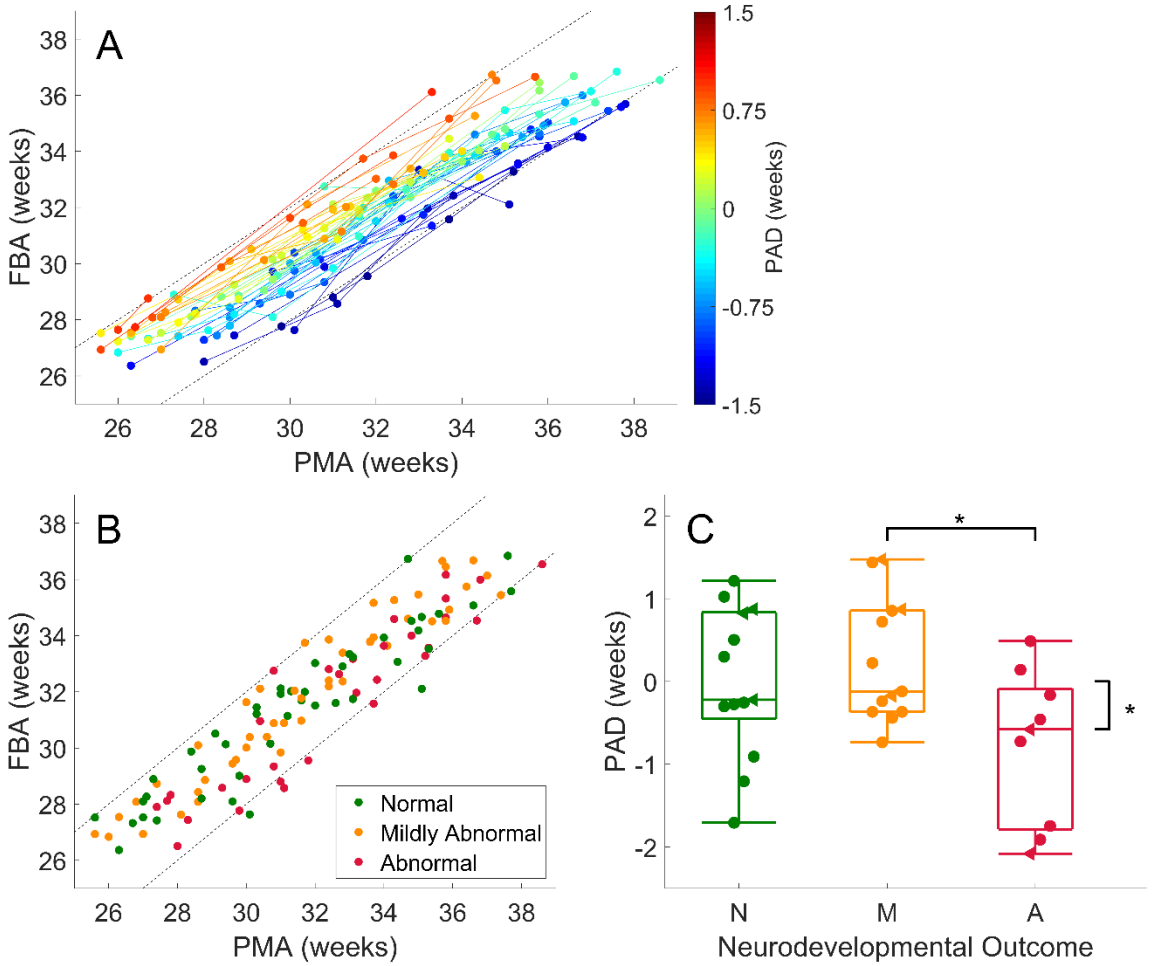

Figure 4: Functional brain age prediction using a multivariable model of quantitative EEG measures. (**A**) Maturational trajectories of individual infants, with at least two serial recordings per infant; $n = 54$, colored according to the average differences between FBA and PMA (PAD: predicted age difference) in each infant. The color bar denotes the PAD in weeks. (**B**) Scatter plot of the subgroup of data, with at least three serial recordings, used to evaluate the prediction error for outcome prediction; $n = 35$, colored according to neurodevelopmental outcome. Straight dashed lines denote a difference of plus or minus 2 weeks between PMA and predicted age. (**C**) Subgroup analysis of EEG predicted age minus PMA with respect to outcome was graded as N – normal (minimum Bayley's score > 85), M – mildly abnormal (minimum Bayley's score between 70 and 85) and A – abnormal (minimum Bayley's score < 70). The asterisks denote $p < 0.05$ between outcome groups and when testing each outcome group against a null hypothesis of zero mean EEG maturity. Data points in have been shifted for clarity of presentation and are denoted with filled circles. Data points represented by triangles are infants with intra-ventricular hemorrhage.

Discussion

The brain matures rapidly in early life with a wide range of structural and functional indices changing over time spans as short as a few weeks. Here, we showed that automated analysis of preterm EEG can be used to track maturation of cortical function with high accuracy. This multivariable prediction of age from the EEG enables the estimation of functional brain maturity to within 1-2 weeks of PMA; an accuracy that generalized to an independent validation dataset acquired under a considerably different EEG recording environment. The margin of error is far lower than similar predictions in preterm infants based on functional neuroimaging with fMRI (*31*), and orders of magnitude lower than what is achieved over later stages of life using EEG or MRI (error margins of 5-10 years) (*32- 34*). Our findings are also comparable to an array of somatic anatomical methods over similar preterm age ranges based on measures of femur length, head circumference, weight, and structural MRI (cortical folding, thickness) (*35-38*). This supports the concept of rapid and distinct changes in anatomy and physiology throughout the preterm period and suggests that physiological and anatomical growth are strongly intertwined (*23, 26, 39*).

The multivariable model developed here advances previous work that was designed to capture key visual elements of EEG review for age prediction. Incorporating burst measures based on the analysis of crackling noise resulted in the most accurate single variable model, improved multivariable model accuracy, and provided a potential framework to explain the mechanistic origins of rapidly evolving preterm EEG signals. The existence of asymmetric burst shapes replicates our previous findings in independent datasets when identifying pathological changes in the EEG at or near birth (*25, 30*). We also validated several recently proposed qEEG variables of maturation: suppression curve, mPLI, global ASI, multi-scale entropy, and path length (coherence) as excellent predictors of age prediction in the preterm period. This supports the use of automated measures of EEG (qEEG) for the extraction of useful information in excess of visual interpretation.

We also successfully validated the model's robustness on unseen data. This showed that the prediction accuracy of the multivariable model holds when translating to a dataset collected within a different clinical environment and with different recording parameters (e.g. amplifier, electrode type, number, and location). This is a crucial hurdle for the clinical translation of new methods, which is impossible to establish in a dataset acquired under uniform conditions. Notably, the independent validation dataset was collected using a 4-channel recording montage

that is commonly used in brain monitoring with the amplitude integrated EEG (*40-42*). This validation on heterogeneous data establishes the wider clinical applicability of determining functional brain age from EEG.

Various measures of growth are commonly used in health care. The finding that neurological dysfunction manifests as immaturity in the EEG is intuitively appealing, and indeed, has been a cornerstone of clinical EEG review for decades (*5, 43-45*). This hypothesis can only be accurately tested with qEEG measures that are strongly correlated with age. We show that most phenomenological measures used in clinical EEG research, such as inter-burst interval, EEG amplitude, or spectral power, are only weakly correlated with age, which challenges their applicability for maturational EEG assessment. We show that more recently proposed qEEG measures (such as asymmetry and sharpness of burst shape, suppression curve, mPLI, MSE, and path length) and multivariable models of age are strongly correlated with PMA and, therefore, more relevant for maturational analyses.

We show that infants follow individual functional maturation trajectories in a highly predictable manner. Analysis of these trajectories with measures such as PAD (the difference between FBA and PMA) can be used to predict neurodevelopmental outcome. We used serial EEG recordings to identify persistent PADs. This suggests that early neurological adversities become embedded in cortical function (EEG recordings), accumulating steadily over the course of neurodevelopmental (*46*). It would be clinically useful to assess whether single PAD measurements at a later stage such as term equivalent age, can provide a sufficiently accurate prediction of future outcomes and, hence, an important proxy for accumulated developmental adversities.

Limited sample sizes, a reality when studying critically ill infants, mean that the reported links between PAD and outcome cannot take into account the variety of factors that may confound this result such as physiological challenges, routine cares, and interventions experienced by preterm infants during their stay in intensive care. These factors will also confound the FBA. There is evidence to suggest that several of these challenges, interventions (many which are designed to accelerate maturation), and other relevant clinical variables can influence EEG activity and, therefore, contribute to variability in the FBA and, therefore, PAD. These variables include the difference between GA and PMA (intra-uterine vs extra-uterine maturation), post-natal adaption, medications, ventilation, birthweight, kangaroo care/infant massage, and gender (*47-56*). We aim to investigate these effects in future work to differentiate

them from other potential causes of inter-subject variability such as natural variability in the course of in-utero growth (*57*). Nevertheless, FBA provides an accurate prediction of PMA even when based on a small training sample with an array of potentially confounding factors that were not explicitly modelled.

The clinical value of FBA is twofold. First, tracking of individual growth trajectories is becoming an important part of individualized medicine for preterm infants (*58-60*). Tracking FBA provides a crucial functional complement to anatomical growth charts, being sensitive to the functional consequence of perinatal adversities specific to early neurological development. Second, these analyses may have an important role in clinical trials, as recent progress in early therapeutic interventions has been hampered by delays due to the assessment of outcome several years after birth. The use of very early measures of neurodevelopmental, like FBA, could lead to dramatically expedited study cycles by allowing more dynamic, adaptive study designs with optimized sample sizes and research questions (*61*). The estimation of FBA also has clear applications in developmental neuroscience, where the assessment of maturation based on cortical function can be used to benchmark models of early human neurological development across species and within human brain organoids (*62*, *63*).

Materials and Methods

Data Acquisition

The training dataset consisted of 67 preterm infants admitted to the NICU at the Vienna General University Hospital, Austria (see Table 2). Infants were included if they were born before 29 weeks of gestational age (GA) and parental consent was received. EEG was acquired with nine scalp electrodes using a Brain Quick / ICU EEG (MicroMed, Treviso, Italy) at a sampling frequency of 256 Hz. Electrode positions reflect the 10-20 international system (modified for neonates) and were located at Fp1, Fp2, C3, C4, T3, T4, O1, O2, with a reference at Cz. A bipolar montage (double banana) was used in analysis: Fp1-C3, C3-O1, Fp1-T3, T3-O1, Fp2-C4, C4-O2, Fp2-T4, T4-O2 (Fig. S1). The EEG was recorded as soon as possible after birth and at fortnightly intervals until term equivalent age, where possible.

Each EEG recording was split into 1 h epochs (with a 75% overlap). Epochs with excessive artefact were excluded from further analysis (see Table 2). GA was defined according to the last menstrual period (LMP). If the LMP-based assessment of gestation deviated considerably from ultrasound findings in the first trimester, ultrasound measurements were used as a

surrogate measure of LMP. PMA, defined as the sum of GA and postnatal age, was used as the benchmark, true age of an infant.

The neurodevelopmental outcome of infants was assessed at ages 1 y and 2 y (Bayley Scales of Infant Neurodevelopment II and III - BII and BIII, respectively; assessed against German norms). Of the 67 preterm infants initially included in the study, 2 were assessed with BII at 1 y, 19 were assessed with BII at 2 y, 35 were assessed with BIII at 2 y, and 11 infants were not assessed for neurodevelopmental outcome. Infants were stratified according to outcome using the following rules applied to the latest available assessment (either 1 y or 2 y): normal (mental developmental index and physical developmental index > 85 [scale II]; or cognitive index, language index, and motor index > 85 [scale III]), or abnormal (either mental developmental index or physical developmental index <70 [scale II]; or either cognitive index, language index, or motor index < 70 [scale III]). Those infants with intermediate scores that did not fit into the normal or abnormal categories were categorized as mildly abnormal.

A summary of the database before and after the rejection of artefactual epochs is presented in Table 2. Data collection was approved by the local ethics committee and written, informed, parental consent was received for each infant included in the database (Medical University Vienna, Austria; study protocol EK Nr 67/2008).

Data Acquisition for Independent, Validation Dataset

We used an independent dataset to validate the single and multivariable models of age prediction. This validation dataset contained EEG recordings from 43 neonates admitted to the NICU at the Wilhelmina Children's Hospital, Utrecht, Netherlands. The data were collected as part of a multi-center European study (*65*). Infants were included in this study if they were born less than 28 weeks GA and informed, written parental consent was received. Infants were excluded if the presence of chromosomal or congenital abnormalities were identified and if the neuro-monitoring was performed with devices other than the BrainZ BRM3 monitor (Natus Medical Incorporated, Seattle, USA). Long duration EEG recordings (~72 h) were recorded as close as possible to admission, followed by shorter recordings (~4-6h) at weekly intervals (up to a post-natal age of approximately four weeks). EEG was recorded with a BrainZ BRM3 monitor and needle electrodes at a sampling frequency of 256 Hz. Two derivations were recorded and used in the analysis: F4-P4 and F3-P3. All neonates had a neurological examination and psychological testing at 30 months of corrected age (Bayley Scales of Infant and Toddler Development III; assessed against Dutch norms). Neonates with normal

neurodevelopmental outcome at this age were included in the validation cohort (normal was defined as per the Vienna dataset; n = 43 infants satisfied these criteria). The data collection protocol was approved by the local medical ethics committee.

Table 2: A summary of infants and EEG recordings before and after application of artefact rejection. Percentages refer to the number of infants/recordings/1 h epochs that were in the initial set that passed the artefact rejection stage. For intraventricular hemorrhage and periventricular leukomalacia, roman numerals indicate increasing grades of severity; assessed by cranial ultrasound and classified according to (*64*). Values are presented as median (interquartile range) where applicable.

Development: Vienna	Initial	post-artefact rejection
gestational age (weeks)	25.3 (24.5-27.0)	25.3 (24.5-27.0)
birthweight (g)	707 (605-920)	704 (604-922)
PMA of EEG recording		
1st	27.0 (26.6-29.4; n=67)	27.9 (26.7-29.6; n=52)
2nd	30.8 (29.2-31.8; n=59)	31.0 (29.5-31.8; n=43)
3rd	33.7 (32.0-34.4; n=54)	33.6 (32.0-34.4; n=46)
4th	35.3 (33.1-36.4; n=37)	35.2 (34.1-36.0; n=36)
5th	36.5 (35.2-37.4; n=16)	36.4 (34.9-36.7; n=9)
6th	38.6 (n=1)	38.6 (n=1)
intraventricular hemorrhage	14 (I/II=10, III/IV=4)	14 (I/II=10, III/IV=4)
periventricular leukomalacia	2 (I/II=2)	1 (I/II=1)
necrotizing enterocolitis	3	3
chronic lung disease	19	19
patent ductus arteriosus	49	48

	infants	recordings	1 h epochs
initial	67	234	1686
post-EEG assessment	65	177	1137
outcome			
normal	20 (100%)	57 (76%)	376 (65%)
mildly abnormal	18 (95%)	57 (78%)	338 (73%)
abnormal	16 (94%)	41 (75%)	238 (62%)
unknown	11 (100%)	22 (71%)	185 (71%)

Validation: Utrecht	initial	post-EEG assessment
gestational age (weeks)	26.9 (26.0-27.6)	26.9 (26.1-27.6)
birthweight (g)	920 (830-1068)	920 (830-1070)
infants	43	42
recordings	105	99
1 h epochs	6561	6101

Prediction of Post-Menstrual Age using qEEG

EEG recorded in an intensive care environment is prone to contamination from electrical activity that is not cortical in origin. All data were high pass filtered with a high pass filter (Butterworth, 4th order, cutoff frequency at 0.5Hz) and then a low-pass filter (Butterworth, 6th order, cutoff frequency at 16 Hz) to eliminate high frequency activity that is more commonly associated with artefacts, including muscle activity (*66*). EEG recordings were then segmented into 1 h epochs. Epochs were scrutinized for further artefacts and were ignored if there was significant spatial differences in amplitude, and if the amplitude was too high or too low (see Supplemental Information for details).

Single and multivariable models of PMA were calculated using regression analysis. The qEEG variables used in this study can be grouped into three categories (Fig. S1): phenomenological analysis (m = 46), burst analysis (m = 40), and other analysis paradigms (m = 10). Phenomenological analysis extracts qEEG variables that mirror the visual interpretation of the EEG. Burst analysis extracts qEEG variables that identify important characteristics of highly irregular ("crackling") noise, through analysis of EEG bursts. Other advanced analyses extract qEEG variables that represent complex characteristics of the preterm EEG such as entropy, global connectivity, and cross-channel coupling. Details on these qEEG variables can be found in the Supplemental Information and implementations of these analysis methods are available via GitHub (see Code Availability).

Leave-one-subject-out cross-validation was used when generating models with a single or multivariable input and FBA as output. In the case of N subjects (infants), a training set consisting of the burst metrics from N-1 subjects was used to define the model parameters. This model was then applied to the left-out subject to generate a predicted age and, hence, a prediction error. The process was repeated until all subjects had been left out, allowing prediction accuracy to be estimated. Single multivariable model parameters were estimated using support vector regression with a medium Gaussian kernel (a kernel scale of 10, a box constraint equal to the interquartile range of PMA/1.349 and epsilon equal to the box constraint/10). Support vector regression is tolerant of redundant and irrelevant variables; nonetheless, we implemented a process of variable selection to rank the importance of each qEEG variable to the determination of age and to reduce the computational burden of the multivariable model. Backwards selection was used (4-fold cross-validation within the training set), with the mean square error between FBA and PMA as a cost function to be minimized.

Independent Validation

A multivariable model was trained on all available data in the Vienna dataset and then applied to the independent dataset collected at the Wilhelmina Children's Hospital, Utrecht, Netherlands. Adjustments were required to overcome sources of heterogeneity, namely different ranges of PMA and different electrode recording configurations. Exploiting the denser electrode array in the Vienna dataset, we generated a two-channel version of the estimator. It was applied to the sparser 4 electrode bipolar montage that is a standard in the brain monitoring practice, also known by clinicians as amplitude-integrated EEG monitoring (*72*). The multivariable model was trained on the two fronto-central derivations (Fp1-C3, Fp2-C4) of the Vienna dataset and then applied to the F3-P3 and F4-P4 derivations of the Utrecht dataset. This was the closest, spatially, approximation given the available recording configurations of the Vienna dataset. Multivariable model parameters were estimated using support vector regression with a Gaussian kernel (kernel scale = 10, box constraint = interquartile range of PMA/1.349 and epsilon = interquartile range of PMA/13.49). Model efficacy was only compared across a similar PMA range between the two datasets (24-33 weeks PMA). The artefact rejection paradigm applied to the Vienna dataset was also implemented on the Utrecht dataset.

Statistical Analysis

A prediction was made on a 1 h epoch of EEG; if multiple EEG epochs exist per recording then the average predicted age per recording was used. The goodness-of-fit between predicted age (single and multivariable models) and PMA was evaluated using the correlation coefficient (Pearson's) and was used to determine the accuracy of the prediction. The bias, variance, and absolute error between predicted age and PMA were also used as measures of goodness-of-fit (*13*). The use of repeated (serial) measures allowed the application of a linear mixed effects model (LMM) where the model output was a fixed effect and the infant ID was a random effect. The LMM was implemented using the fitlme function in Matlab [pma ~ model output + (1 | infant ID)]. The adjusted r value was used to assess the goodness-of-fit taking into account multiple recordings from each infant. Statistical comparisons of measures of the goodness-of-fit between EEG metrics for the prediction of PMA were performed using resampling methods (bootstrap). A correlation coefficient was deemed significantly different if the 95% confidence interval of differences (estimated via a bootstrap) did not span zero, i.e., was either positive or negative. Differences in prediction accuracy (absolute error) between the Vienna (training) and

Utrecht (validation) sets were evaluated using equivalence testing with a two, one-sided t-tests (TOST) procedure based on Welch's t-test (*73*). We used a mean difference in absolute error of ±0.5 weeks as a conservative equivalence boundary based on the results of previous work which reported an absolute prediction error of approximately ±1 week (*14*). Differences in FBA trajectories (FBA subtracted from PMA and then averaged across all serial recordings) between outcome groups were tested using a one-way ANOVA, with Levene's test for homogeneity of group variances and a post hoc analysis performed using Tukey's Range test to correct for multiple comparisons. Furthermore, FBA trajectories in each group were assessed to determine if they were significantly different from zero using a t-test. For post-hoc analyses, Cohen's D statistic, with small sample size correction, was used to estimate the effect size between groups. All tests were two-tailed and used a level of significance of 0.05.

Data availability

Access to the raw EEG recordings is available at request (LdV and MJNLB for the Utrecht dataset and KKS for the Vienna dataset).

Code availability

Implementations of the analysis methods are available via GitHub - github.com/nstevensonUH/Neonatal-EEG-Analysis/tree/master/Preterm_Features_Literature.

Acknowledgments

This work was supported by the National Health and Medical Research Council of Australia (JAR, MB, SV, PBC, APP1144936; MB, APP1118153), the Rebecca L. Cooper Foundation (JAR, PG2018109), Lastentautiensäätiö (SV), the Finnish Academy (SV, 313242, 288220), Fonds zur Förderung der Wissenschaftlichen Forschung (KKS, FWFKLI237) and the European Commission (LdV, MJNLB; LSHM-CT-2006-036534).

Author contributions

NJS, SV and JAR contributed to study conceptualization; NJS, JAR and SV undertook preliminary investigations, NJS performed the formal analysis; LO, MLT, LdV, KKS, SV contributed to data collection and curation; JAR, MB, SV, and PBC acquired funding for the study; and all authors contributed to the writing of the paper.

Competing interests: JAR, MB, and SV have a pending patent application on the burst metrics used in this paper. The authors declare no other competing interests.

Supplementary Information

Fig. S1: Analysis overview. Estimating FBA from the EEG signal using a 'bag of features' combined using kernel support vector regression.

Fig. S2: Variable selection in a multivariable model of post-menstrual age based on qEEG analysis.

Fig. S3: The number of EEG epochs rejected as artefactual compared to a visual interpretation of the level of contamination by artefact.

Table S1: Correlation between single variable predictions based on a single qEEG variables and PMA within a leave-one-subject-out cross-validation.

Table S2: Differences in prediction accuracy from increasing the training data with infants with non-optimal outcome.

References

1. Costeloe KL, Hennessy EM, Haider S, Stacey F, Marlow N, Draper ES. Short term outcomes after extreme preterm birth in England: comparison of two birth cohorts in 1995 and 2006 (the EPICure studies). British Medical Journal. **345,** e7976 (2012).
2. Saigal S, Doyle LW. An overview of mortality and sequelae of preterm birth from infancy to adulthood. The Lancet. **371**, 261-269 (2008).
3. Gluckman PD, Hanson MA, Cooper C, Thornburg KL. Effect of in utero and early-life conditions on adult health and disease. New England Journal of Medicine. **359**, 61-73 (2008).
4. Woodward LJ, Anderson PJ, Austin NC, Howard K, Inder TE. Neonatal MRI to predict neurodevelopmental outcomes in preterm infants. New England Journal of Medicine. **355**, 685-694 (2006).
5. Watanabe K, Hayakawa F, Okumura A. Neonatal EEG: a powerful tool in the assessment of brain damage in preterm infants. Brain and Development. **21**, 361-72 (1999).
6. Hayashi-Kurahashi N, Kidokoro H, Kubota T, Maruyama K, Kato Y, Kato T, Natsume J, Hayakawa F, Watanabe K, Okumura A. EEG for predicting early neurodevelopment in preterm infants: an observational cohort study. Pediatrics. **130**, e891-e897 (2012).

7. Wikström S, Pupp IH, Rosén I, Norman E, Fellman V, Ley D, Hellström-Westas L. Early single-channel aEEG/EEG predicts outcome in very preterm infants. Acta Paediatrica. **101**, 719-726 (2012).
8. Fogtmann EP, Plomgaard AM, Greisen G, Gluud C. Prognostic accuracy of electroencephalograms in preterm infants: a systematic review. Pediatrics. **139**, e20161951 (2017).
9. Lloyd RO, O'Toole JM, Livingstone V, Hutch WD, Pavlidis E, Cronin AM, Dempsey EM, Filan PM, Boylan GB. Predicting 2-y outcome in preterm infants using early multimodal physiological monitoring. Pediatric research. **80**, 382-388 (2016).
10. Dempsey EM, Kooi EM, Boylan G. It's All About the Brain-Neuromonitoring During Newborn Transition. Seminars in Pediatric Neurology. **28**, 48-59 (2018).
11. Hrachovy RA, Mizrahi EM. Atlas of Neonatal Electroencephalography. 4th ed. Deimos Medical Publishing; 2016.
12. Cole JH, Marioni RE, Harris SE, Deary IJ. Brain age and other bodily 'ages': implications for neuropsychiatry. Molecular Psychiatry. **24,** 266–281 (2019)
13. O'Toole JM, Boylan GB, Vanhatalo S, Stevenson NJ. Estimating functional brain maturity in very and extremely preterm neonates using automated analysis of the electroencephalogram. Clinical Neurophysiology. **127**, 2910-2918 (2016).
14. Stevenson NJ, Oberdorfer L, Koolen N, O'Toole JM, Werther T, Klebermass-Schrehof K, Vanhatalo S. Functional maturation in preterm infants measured by serial recording of cortical activity. Scientific Reports. **7**, 12969 (2017).
15. Roberts JA, Iyer KK, Finnigan S, Vanhatalo S, Breakspear M. Scale-free bursting in human cortex following hypoxia at birth. Journal of Neuroscience. **34**, 6557-6572 (2014).
16. Dereymaeker A, Koolen N, Jansen K, Vervisch J, Ortibus E, De Vos M, Van Huffel S, Naulaers G. The suppression curve as a quantitative approach for measuring brain maturation in preterm infants. Clinical Neurophysiology. **127**, 2760-2765 (2016).
17. Van de Pol LA, van't Westende C, Zonnenberg I, Koedam E, van Rossum I, De Haan W, Steenweg M, van Straaten EC, Stam CJ. Strong relation between an EEG functional connectivity measure and postmenstrual age: a new potential tool for measuring neonatal brain maturation. Frontiers in Human Neuroscience. **12**, 286 (2018).
18. De Wel O, Lavanga M, Dorado AC, Jansen K, Dereymaeker A, Naulaers G, Van Huffel S. Complexity analysis of neonatal EEG using multiscale entropy: applications in brain maturation and sleep stage classification. Entropy. **19**, 516 (2017).

19. Lavanga M, De Wel O, Caicedo A, Jansen K, Dereymaeker A, Naulaers G, Van Huffel S. A brain-age model for preterm infants based on functional connectivity. Physiological Measurement. **39**, 044006 (2018).
20. Tokariev A, Roberts JA, Zalesky A, Zhao X, Vanhatalo S, Breakspear M, and Cocchi L. Large-scale brain modes reorganize between infant sleep states and carry prognostic information for preterms. Nature Communications. **10**, 2619 (2019).
21. Omidvarnia A, Fransson P, Metsäranta M, Vanhatalo S. Functional bimodality in the brain networks of preterm and term human newborns. Cerebral Cortex. **24**, 2657-68 (2013).
22. Khazipov R, Luhmann HJ. Early patterns of electrical activity in the developing cerebral cortex of humans and rodents. Trends in Neurosciences. **29**, 414-418 (2006).
23. Luhmann HJ, Sinning A, Yang JW, Reyes-Puerta V, Stüttgen MC, Kirischuk S, Kilb W. Spontaneous neuronal activity in developing neocortical networks: from single cells to large-scale interactions. Frontiers in Neural Circuits. **10**, 40 (2016)
24. Omidvarnia A, Metsäranta M, Lano A, Vanhatalo S. Structural damage in early preterm brain changes the electric resting state networks. NeuroImage 120, 266-73 (2015).
25. Iyer KK, Roberts JA, Hellström-Westas L, Wikström S, Hansen-Pupp I, Ley D, Vanhatalo S, Breakspear M. Cortical burst dynamics predict clinical outcome early in extremely preterm infants. Brain. **138**, 2206-18 (2015).
26. Tataranno ML, Claessens NH, Moeskops P, Toet MC, Kersbergen KJ, Buonocore G, Išgum I, Leemans A, Counsell S, Groenendaal F, De Vries LS, Benders MJNL. Changes in brain morphology and microstructure in relation to early brain activity in extremely preterm infants. Pediatric Research. **83**, 834-842 (2018).
27. Sethna JP, Dahmen KA, Myers CR. Crackling noise. Nature. **410**, 242-250 (2001)
28. Roberts J A, Boonstra, TW, Breakspear M. The heavy tail of the human brain. Current Opinion in Neurobiology, **31**, 164-172 (2015).
29. Iyer KK, Roberts JA, Metsäranta M, Finnigan S, Breakspear M, Vanhatalo S. Novel features of early burst suppression predict outcome after birth asphyxia. Annals of Clinical and Translational Neurology. **1**, 209-14 (2014).
30. Iyer KK, Roberts JA, Hellström-Westas L, Wikström S, Hansen-Pupp I, Ley D, Breakspear M, Vanhatalo S. Early detection of preterm intraventricular hemorrhage from clinical electroencephalography. Critical Care Medicine. **43**, 2219-2227 (2015).
31. Smyser CD, Dosenbach NU, Smyser TA, Snyder AZ, Rogers CE, Inder TE, Schlaggar BL, Neil JJ. Prediction of brain maturity in infants using machine-learning algorithms. NeuroImage. **136**, 1-9 (2016).

32. Franke K, Ziegler G, Klöppel S, Gaser C, Estimating the age of healthy subjects from T1-weighted MRI scans using kernel methods: exploring the influence of various parameters. NeuroImage. **50**, 883-892 (2010).
33. Sun H, Paixao L, Oliva JT, Goparaju B, Carvalho DZ, van Leeuwen KG, Akeju O, Thomas RJ, Cash SS, Bianchi MT, Westover MB. Brain age from the electroencephalogram of sleep. Neurobiology of Aging. **74**, 112-120 (2019).
34. Al Zoubi O, Ki Wong C, Kuplicki RT, Yeh HW, Mayeli A, Refai H, Paulus M, Bodurka J. Predicting Age From Brain EEG Signals—A Machine Learning Approach. Frontiers in Aging Neuroscience. (2018) doi: 10.3389/fnagi.2018.00184
35. Dubowitz LM, Dubowitz V, Goldberg C Clinical assessment of gestational age in the newborn infant. Journal of Pediatrics. **77**, 1-10 (1970).
36. Shimony JS, Smyser CD, Wideman G, Alexopoulos D, Hill J, Harwell J, Dierker D, Van Essen DC, Inder TE, Neil JJ. Comparison of cortical folding measures for evaluation of developing human brain. NeuroImage. **125**, 780-790 (2016).
37. Biagioni E, Frisone MF, Laroche S, Kapetanakis BA, Ricci D, Adeyi-Obe M, Lewis H, Kennea N, Cioni G, Cowan F, Rutherford M. Maturation of cerebral electrical activity and development of cortical folding in young very preterm infants. Clinical Neurophysiology. **118**, 53-59 (2007).
38. Lefèvre J, Germanaud D, Dubois J, Rousseau F, de Macedo Santos I, Angleys H, Mangin JF, Hüppi PS, Girard N, De Guio F. Are developmental trajectories of cortical folding comparable between cross-sectional datasets of fetuses and preterm newborns? Cerebral Cortex. **26**, 3023-3035 (2015).
39. Benders MJ, Palmu K, Menache C, Borradori-Tolsa C, Lazeyras F, Sizonenko S, Dubois J, Vanhatalo S, Hüppi PS. Early brain activity relates to subsequent brain growth in premature infants. Cerebral Cortex. **25**, 3014-3024 (2014).
40. Shah NA, Wusthoff CJ. How to use: amplitude-integrated EEG (aEEG). Archives of Disease in Childhood: Education and Practice Edition. **100**, 75-81 (2015).
41. Reynolds LC, Pineda RG, Mathur A, Vavasseur C, Shah DK, Liao S, Inder T. Cerebral maturation on amplitude-integrated electroencephalography and perinatal exposures in preterm infants. Acta Paediatrica. **103**, e96-100, (2014).
42. Olischar M, Klebermass K, Kuhle S, Hulek M, Kohlhauser C, Rücklinger E, Pollak A, Weninger M. Reference values for amplitude-integrated electroencephalographic activity in preterm infants younger than 30 weeks' gestational age. Pediatrics. **113**, e61-e66 (2004).

43. Parmelee Jr AH, Schulte FJ, Akiyama Y, Wenner WH, Schultz MA, Stern E. Maturation of EEG activity during sleep in premature infants, Electroencephalography and Clinical Neurophyiology, **24**, 319-329 (1968).
44. Scher MS. Neurophysiological assessment of brain function and maturation II. A measure of brain dysmaturity in healthy preterm neonates. Pediatric Neurology. **16**, 287-95 (1997).
45. Holthausen K, Breidbach O, Scheidt B, Frenzel J. Brain dysmaturity index for automatic detection of high-risk infants. Pediatric Neurology. **22**, 187-91 (2000).
46. Hanson MA, Gluckman PD. Early developmental conditioning of later health and disease: physiology or pathophysiology? Physiological Reviews. **94**, 1027-76 (2014).
47. Soubasi V, Mitsakis K, Nakas CT, Petridou S, Sarafidis K, Griva M, Agakidou E, Drossou V. The influence of extrauterine life on the aEEG maturation in normal preterm infants. Early Hum Development. **85**, 761-765 (2009).
48. Klebermass K, Kuhle S, Olischar M, Rücklinger E, Pollak A, Weninger M. Intra-and extrauterine maturation of amplitude-integrated electroencephalographic activity in preterm infants younger than 30 weeks of gestation. Neonatology. **89**, 120-125 (2006).
49. Guzzetta A, D'Acunto MG, Carotenuto M, Berardi N, Bancale A, Biagioni E, Boldrini A, Ghirri P, Maffei L, Cioni G. The effects of preterm infant massage on brain electrical activity. Developmental Medicine and Child Neurology. **53**, 46-51 (2011).
50. Bell AH, Greisen G, Pryds O. Comparison of the effects of phenobarbitone and morphine administration on EEG activity in preterm babies. Acta Paediatrica. **82**, 35-39 (1993).
51. Malk K, Metsäranta M, Vanhatalo S. Drug effects on endogenous brain activity in preterm babies. Brain and Development. **36**, 116-123 (2014)
52. Pavlidis E, Lloyd RO, Boylan GB. EEG-a valuable biomarker of brain injury in preterm infants. Developmental Neuroscience. **39**, 23-35 (2017).
53. Nunes ML, Khan RL, Gomes Filho I, Booij L, da Costa JC. Maturational changes of neonatal electroencephalogram: a comparison between intra uterine and extra uterine development. Clinical Neurophysiology. **125**, 1121-1128 (2014).
54. Natalucci G, Hagmann C, Bernet V, Bucher HU, Rousson V, Latal B. Impact of perinatal factors on continuous early monitoring of brain electrocortical activity in very preterm newborns by amplitude-integrated EEG. Pediatric Research. **75**, 774-780 (2014).
55. O'Toole JM, Pavlidis E, Korotchikova I, Boylan GB, Stevenson NJ. Temporal evolution of quantitative EEG within 3 days of birth in early preterm infants. Scientific Reports. **9**, 4859 (2019).

56. Griesmaier E, Santuari E, Edlinger M, Neubauer V, Waltner-Romen M, Kiechl-Kohlendorfer U. Differences in the maturation of amplitude-integrated EEG signals in male and female preterm infants. Neonatology. **105**, 175-181 (2014).
57. Guihard-Costa AM, Droullé P, Thiebaugeorges O, Hascoet JM. A longitudinal study of fetal growth variability. Neonatology. **78**, 8-12 (2000).
58. Rochow N, Raja P, Liu K, Fenton T, Landau-Crangle E, Göttler S, Jahn A, Lee S, Seigel S, Campbell D, Heckmann M. Physiological adjustment to postnatal growth trajectories in healthy preterm infants. Pediatric Research. **79**, 870-879 (2016).
59. Raghuram K, Yang J, Church PT, Cieslak Z, Synnes A, Mukerji A, Shah PS, Canadian Neonatal Network, Canadian Neonatal Follow-Up Network Investigators. Head growth trajectory and neurodevelopmental outcomes in preterm neonates. Pediatrics. **140**, e20170216 (2017).
60. Landau-Crangle E, Rochow N, Fenton TR, Liu K, Ali A, So HY, Fusch G, Marrin ML, Fusch C. Individualized postnatal growth trajectories for preterm infants. Journal of Parenteral and Enteral Nutrition. **42**, 1084-1092 (2018).
61. Pedroza C, Tyson JE, Das A, Laptook A, Bell EF, Shankaran S. Advantages of Bayesian monitoring methods in deciding whether and when to stop a clinical trial: an example of a neonatal cooling trial. Trials. **17**, 335 (2016).
62. Clancy B, Finlay BL, Darlington RB, Anand KJ. Extrapolating brain development from experimental species to humans. Neurotoxicology. **28**, 931-937 (2007).
63. Trujillo CA, Gao R, Negraes PD, Gu J, Buchanan J, Preissl S, Wang A, Wu W, Haddad GG, Chaim IA, Domissy A. Complex Oscillatory Waves Emerging from Cortical Organoids Model Early Human Brain Network Development. Cell Stem Cell. (2019) doi: 10.1016/j.stem.2019.08.002.
64. Papile LN, Burnstein J, Burnstein R, Koffler H: Incidence and evolution of subeoendymal and intraventricular hemorrhage: a study of infants with birthweight less than 1500g. Journal of Pediatrics. **92**:529-534 (2007)
65. Dammann O, Cesario A, Hallen M. NEOBRAIN–An EU-Funded Project Committed to Protect the Newborn Brain. Neonatology. **92**: 217-218 (2007).
66. Norman E, Rosén I, Vanhatalo S, Stjernqvist K, Ökland O, Fellman V, Hellström-Westas L. Electroencephalographic response to procedural pain in healthy term newborn infants. Pediatric Research. **64**, 429-434 (2008).
67. Reilly A, Frazer G, Boashash B. Analytic signal generation-tips and traps. IEEE Transactions on Signal Processing. **42**, 3241-3245 (1994).

68. Vanhatalo S, Kaila K. Spontaneous and evoked activity in the early human brain. *In. The Newborn Brain: Neuroscience & Clinical Applications* 2nd edition (Eds. H. Lagercrantz, MA Hanson, LR Ment, DM Peebles) Cambridge University Press, Chapter 15, 229-243 (2010).
69. O'Reilly D, Navakatikyan MA, Filip M, Greene D, Van Marter LJ. Peak-to-peak amplitude in neonatal brain monitoring of premature infants. Clinical Neurophysiology. **123**, 2139-2153 (2012).
70. Koolen N, Dereymaeker A, Räsänen O, Jansen K, Vervisch J, Matic V, Naulaers G, De Vos M, Van Huffel S, Vanhatalo S. Early development of synchrony in cortical activations in the human. Neuroscience. **322**, 298-307 (2016).
71. Schetinin V, Jakaite L. Extraction of features from sleep EEG for Bayesian assessment of brain development. PLoS One. **12**, e0174027 (2017).
72. Griesmaier E, Enot DP, Bachmann M, Neubauer V, Hellström-Westas L, Kiechl-Kohlendorfer U, Keller M. Systematic characterization of amplitude-integrated EEG signals for monitoring the preterm brain. Pediatric Research. **73**, 226-235 (2013).
73. Lakens D. Equivalence tests: a practical primer for t tests, correlations, and meta-analyses. Social Psychological and Personality Science. **8**, 355-362 (2017)
74. Palmu K, Stevenson N, Wikström S, Hellström-Westas L, Vanhatalo S, Palva JM. Optimization of an NLEO-based algorithm for automated detection of spontaneous activity transients in early preterm EEG. Physiological Measurement. **31**, N85-N93 (2010).